Development 139, 2351-2359 (2012) doi:10.1242/dev.078485
© 2012. Published by The Company of Biologists Ltd

# FGF signaling establishes the anterior border of the *Ciona* neural tube

**Eileen Wagner* and Michael Levine**

## SUMMARY

The *Ciona* tadpole is constructed from simple, well-defined cell lineages governed by provisional gene networks that have been defined via extensive gene disruption assays. Here, we examine the patterning of the anterior neural plate, which produces placodal derivatives such as the adhesive palps and stomodeum, as well as the sensory vesicle (simple brain) of the *Ciona* tadpole. Evidence is presented that the *doublesex*-related gene *DMRT* is expressed throughout the anterior neural plate of neurulating embryos. It leads to the activation of *FoxC* and *ZicL* in the palp placode and anterior neural tube, respectively. This differential expression depends on FGF signaling, which inhibits *FoxC* expression in the anterior neural tube. Inhibition of FGF signaling leads to expanded expression of *FoxC*, the loss of *ZicL*, and truncation of the anterior neural tube.

**KEY WORDS: *Ciona intestinalis*, FGF/MAPK, FoxC, Neural boundary, Placode**

## INTRODUCTION

The generation of diverse cell types from a fertilized egg remains a fundamental problem for developmental biologists. The simple chordate *Ciona intestinalis* is well suited to address this question owing to its small cell number, detailed cell lineage characterization, experimental tractability and provisional gene regulatory networks (Passamaneck and Di Gregorio, 2005; Satou et al., 2009). *Ciona*, an ascidian, belongs to the urochordates, which represent the closest living relatives of the vertebrates (Delsuc et al., 2006). Ascidians are sessile, filter-feeding animals with incurrent and excurrent siphons that develop following the settlement and metamorphosis of a swimming tadpole larva. Ascidians diverged from vertebrates before the two rounds of genome duplication that created the large multigene families that complicate genetic analysis in vertebrates (Dehal and Boore, 2005).

The *Ciona* central nervous system (CNS) develops via neurulation of cells within the neural plate, forming a simple brain, which is also called the sensory vesicle, and a caudal nerve cord (Nicol and Meinertzhagen, 1988; Lemaire et al., 2002). *Ciona* also has neurogenic tissues that derive from the anterior neural plate but do not undergo neurulation and instead contribute to the peripheral nervous system (PNS) (Meinertzhagen et al., 2004). The corresponding region in vertebrate embryos forms the anterior placodes, namely the lens, olfactory and adenohypophyseal placodes (Toro and Varga, 2007; Streit, 2008; Schlosser, 2010). The anteriormost neural plate derivatives in *Ciona* are the adhesive papillae, or palps. The palps are three bumps on the rostral end of the tadpole that contain sensory neurons that project to the brain (Imai and Meinertzhagen, 2007b). The palps secrete adhesive substances that secure attachment of the tadpole to a solid substrate in preparation for the metamorphosis that creates the sessile adult body plan. Morphological, embryological and molecular evidence suggest that ascidian palps represent a rudimentary placode (Manni et al., 2004; Mazet et al., 2005). Another placode-like structure, the stomodeum, arises from the neural plate territory sandwiched between the palp placode and the anterior neural tube (Manni et al., 2005; Christiaen et al., 2007). The stomodeum gives rise to the oral siphon (mouth) of the adult and derives from the anterior neuropore (Veeman et al., 2010). In vertebrates, the stomodeum invaginates to form Rathke's pouch and, ultimately, the anterior pituitary.

Fibroblast growth factor (FGF) signaling plays an important role in neural induction and subsequent development throughout the vertebrates (Ribisi et al., 2000; Streit et al., 2000; Dono, 2003; Delaune et al., 2005; Paek et al., 2009). Likewise, the FGF signaling pathway also functions in neural development in ascidians. In *Ciona*, neural induction begins with *Otx* expression at the 32-cell stage in the anterior neurectoderm via GATA and Ets transcription factors in response to FGF signaling (Bertrand et al., 2003). The requirement for FGF signaling persists in later development, when it is required for patterning posterior components of the nervous system (Hudson et al., 2003; Imai et al., 2009; Stolfi and Levine, 2011). Thus, FGF signaling acts at both early and late stages of *Ciona* nervous system development.

Much progress has been made in recent years toward uncovering the gene regulatory networks that control the development of the posterior nervous system. Less is known about the early patterning mechanisms in the anteriormost nervous system. Here, we examine the role of FGF signaling in a cell fate choice between the palp placode and the anterior CNS, which express *FoxC* and *ZicL*, respectively. We find that FGF-MAPK signaling is required to establish the posterior boundary of the *FoxC* expression domain, as abrogation of this pathway results in ectopic *FoxC* expression and loss of CNS markers. We identified an Ets binding site in a minimal *FoxC* enhancer that is required to repress *FoxC* in the CNS progenitors. Strikingly, we observe a truncated anterior neural tube in tailbud stage embryos that experience FGF-MAPK perturbation, as well as a posterior shift in the position of the neuropore. Thus, FGF signaling delineates the boundary between the palp placode and the anterior neural tube.

Center for Integrative Genomics, Division of Genetics, Genomics, and Development, Department of Molecular and Cell Biology, University of California Berkeley, Berkeley, CA 94720, USA.

*Author for correspondence (wagnerem@berkeley.edu)

**Accepted 15 April 2012**

## MATERIALS AND METHODS

### Embryo electroporation

*Ciona intestinalis* adult animals were collected at Pillar Point Harbor in Half Moon Bay, California, or obtained from M-Rep (San Diego, CA, USA). Dechorionation, fertilization and electroporation of eggs were performed as described (Christiaen et al., 2009b; Christiaen et al., 2009c). Each experiment was performed at least twice. Electroporation was with 40-100 μg of each plasmid. Fluorescent images were obtained with a Zeiss Axio Imager.A2 upright fluorescence microscope or a Zeiss 700 laser-scanning confocal microscope.

### Molecular cloning

#### Enhancers

The *DMRT* enhancer was amplified from *Ciona intestinalis* genomic DNA with DMRT –1k PstF (5′-GAAGTACTGCAGTAGTA-GGGTGGAGGAAGATGGGAC) and DMRT NR (5′-AAAGCGGCCGCCATGCCAGTTAAACGAACTGTTTG); underlining indicates restriction sites used for cloning. Enhancers for *FoxC* were isolated with FoxC –2.1 BF (5′-GAAGTAGGATCCGACTTTC-AGGCCGCCTACGTAGGGTAAATA) and FoxC NR (5′-GAAG-TAGCGGCCGCCATTATAGAGAATCAAACCAAGGATTCGGT). The ‘minimal’ *FoxC* enhancer was amplified with FoxC-375XhF (5′-GAAACTCGAGCAGGTGTTTCGTAAGGCGGC) and FoxC –50 BR (5′-TAATGGATCCAACTTACACTAACACTGCCCG). Enhancer fragments were cloned upstream of *lacZ* in the CesA vector (Harafuji et al., 2002) or into modified vectors in which *lacZ* was replaced with GFP, mCherry or derivatives thereof. The *ZicL* –1.5 kb enhancer and the *FoxB* enhancer have been described previously (Shi and Levine, 2008; Imai et al., 2009).

#### Coding sequences

RNA was isolated from staged embryos using Trizol (Invitrogen) and reverse transcribed with oligo(dT) and Superscript II reverse transcriptase (Invitrogen). The *FoxC* coding sequence was amplified with FoxC cds NF (5′-GAAGTAGCGGCCGCAATGACAATGCAAATCCGGTACCCGTC-GTCC) and FoxC cds ER (5′-GAAGTAGAATTCTC-AGTACTTAGTGTAATCGTAAGCAG) and cloned downstream of the *DMRT* enhancer. The *RorA* coding sequence was amplified with RorA NF (5′-GAAGAAGCGGCCGCAATGTTTCGTCATACCGGTTACGTC) and RorA ER (5′-ATAGAATTCCGTGGTCTGGTTTGCATCGCGAC) and cloned into the pCRII (Invitrogen) dual promoter vector to prepare the in situ probe. *ELK* coding sequence oligos were ELK cds PspF (5′-ATAAGGGCCCATGATGACATTGAAAATCGACACAG) and ELK cds MfeR (5′-GAATACAATTGTTACGATGAAGTTAGTGTCGTGACGG). The *ZicL* coding sequence was gift from L. Christiaen (New York University, USA) and subcloned downstream of the *DMRT* enhancer using *Not*I and *Blp*I restriction sites. The DN-FGFR and CA-FGFR transgenes (Davidson et al., 2006; Shi and Levine, 2008) were subcloned downstream of the *DMRT* enhancer by standard methods.

### Site-directed mutagenesis

Ets sites were deleted from the *FoxC* minimal enhancer using the QuikChange Lightning Mutagenesis Kit (Stratagene/Agilent) with delEts-295 F (5′-CATTAGCGCGCCATTGCGCGAAAGTTGATTGG), delEts-295 R (5′-CCAATCAACTTTCGCGCAATGGCGCGCTAATG), delEts-255 F (5′-GATTATGACGCTCCTGCTATTGTTTAAGGGGAGATG) and delEts-255 R (5′-CATCTCCCCTTAAACAATAGCAGGAGCGTC-ATAATC).

### Double in situ hybridization/antibody staining

The following in situ hybridization probes were obtained from plasmids contained in the *Ciona intestinalis* gene collection release I: *FoxC* (GC44e14), *ZicL* (GC08g08), *ELK* (GC27g08), *Ephrin A-d* (GC01j20), *Epi1* (GC25g21) and *Six3/6* (GC11m13). PCR amplification of transcription templates was with the following oligos: BSK-MT (5′-GCAAGGCGATTAAGTTGGGTAACG) and M13R (5′-CAGGAAACAGCTATGAC). DIG-labeled probes were transcribed with T7 RNA polymerase (Roche) using DIG labeling mix (Roche) and purified with the RNeasy Mini Kit (Qiagen).

Double fluorescent in situ hybridization and β-galactosidase (β-gal) antibody staining was performed as follows. Mid-gastrula stage embryos were fixed in MEM-PFA (4% paraformaldehyde, 0.1 M MOPS pH 7.4, 0.5 M NaCl, 1 mM EGTA, 2 mM $MgSO_4$, 0.05% Tween 20) overnight at 4°C. Embryos were rinsed in cold PBS and dehydrated as described (Christiaen et al., 2009d) and kept at –20°C. Prior to rehydration, embryos were treated with 2% $H_2O_2$ in methanol for 30 minutes at room temperature, and then rehydrated and manipulated as described through the post-hybridization washes (Christiaen et al., 2009d). Embryos were then equilibrated in TNT (100 mM Tris pH 7.5, 150 mM NaCl, 0.1% Tween 20) and blocked in TNB (0.5% Roche blocking reagent in 100 mM Tris pH 7.5, 150 mM NaCl) for 1-2 hours. Anti-β-gal (Promega) and anti-DIG-POD (Roche) antibodies were diluted 1:1000 in TNB and incubated with embryos overnight at 4°C. Embryos were washed extensively in TNT. For tyramide signal amplification, Cy3-coupled or fluorescein-coupled TSA Plus reagent (PerkinElmer) was diluted 1:100 in amplification diluent and added to embryos for 5-10 minutes at room temperature. Embryos were washed in TNT and incubated with secondary antibody (anti-mouse Alexa Fluor 488 or Alexa Fluor 555, Molecular Probes) at 1:1000 dilution overnight at 4°C. Embryos were washed in TNT and equilibrated and mounted in 50% glycerol in PBS containing 2% DABCO (Sigma).

### Drug treatments

The MEK inhibitor U0126 (Promega) was resuspended in DMSO to prepare a 10 mM stock, and diluted in filtered artificial sea water (FASW) to 10 μM working concentration. Embryos at the 76-cell stage were transferred to FASW containing U0126 or DMSO as control.

### Embryo manipulation

For antibody staining, embryos were fixed in MEM-FA (3.7% methanol-free formaldehyde, 0.1 M MOPS pH 7.4, 0.5 M NaCl, 2 mM $MgSO_4$, 1 mM EGTA) for 30 minutes, rinsed several times in PBT (PBS with 0.1% Tween 20), and incubated with anti-dpERK antibody (Sigma M9692) at 1:1000 with 2% normal donkey serum (NDS) in PBT at 4°C overnight. Embryos were washed in PBT and then incubated with donkey anti-mouse secondary antibody (1:1000) coupled to Alexa Fluor 555 (Molecular Probes) in PBT with 2% NDS for 2 hours at room temperature, then washed in PBT. For phalloidin staining, phalloidin (Molecular Probes) was diluted 1:500 in PBT, and embryos were incubated for 2-4 hours at room temperature, followed by PBT washes. For Hoechst staining, Hoechst (Molecular Probes) was diluted 1:1000 in PBT, and embryos were incubated for 0.5-2 hours, then washed in PBT. All embryos were equilibrated and mounted in 50% glycerol in PBS containing 2% DABCO.

## RESULTS

Neurons of the swimming tadpole can be traced to individual blastomeres in the neural plate, which reflect the ascidian lineage-based cell nomenclature of Conklin (Conklin, 1905). The neural plate in *Ciona* emerges at the mid-gastrula stage on the dorsal surface of the embryo in a characteristic grid of cells with eight columns and six rows (our schematic in Fig. 1B is simplified to exclude the lateral-most columns that derive from the posterior ectoderm). The posterior neural plate, comprising rows I and II, derives from the anterior vegetal lineage (denoted as A-line) and contribute to the caudal nerve cord, motor ganglion and posterior sensory vesicle (we use the term posterior brain for simplicity) (Imai et al., 2009). Cells in rows III-VI derive from the anterior ectodermal lineage known as the a-line. Progeny of row III contribute to the anterior sensory vesicle (hereafter called anterior brain), whereas cells of row IV contribute to the stomodeum as well as the anterior brain. Rows V and VI comprise the anteriormost neural plate, and the progeny of these cells contribute to the palps as well as to epidermal sensory neurons in the trunk (see Fig. 1B,D). It is prudent to note that the derivatives of rows V/VI generate neurons of the PNS, and that the CNS derives from cells in rows I-IV, which undergo primary neurulation. In

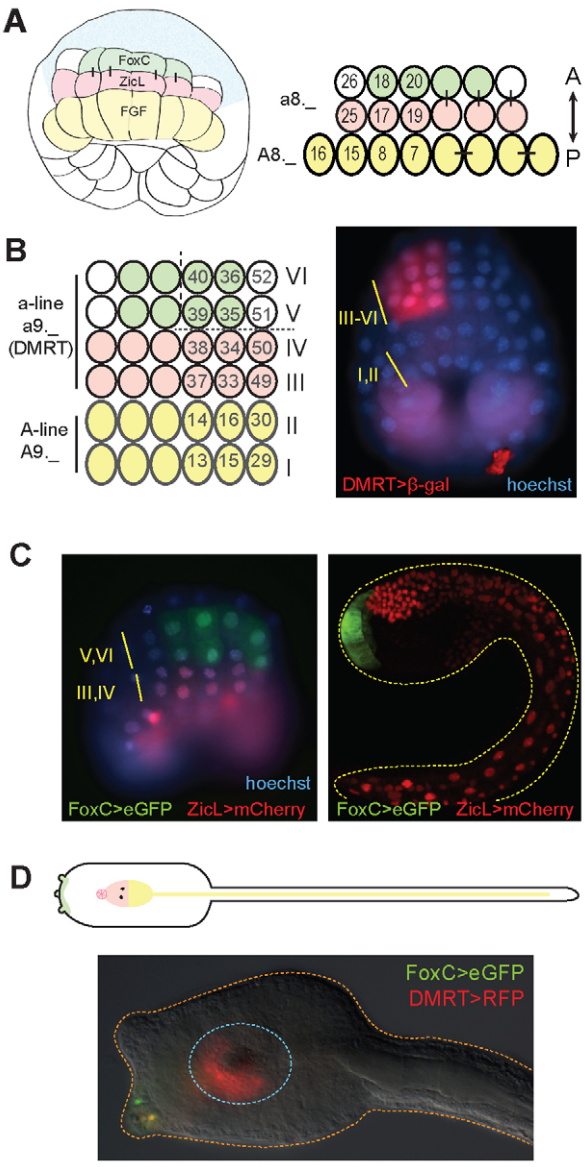


**Fig. 1. The *Ciona* neural plate and palp placode.** (**A**) (Left) Schematic of a 112-cell embryo showing *FoxC*-expressing cells (green) and their sister cells that express *ZicL* (pink). The A-line (vegetal) neural precursors (yellow) express FGF9/16/20. Non-neural ectoderm is in blue. (Right) Cells of the nascent neural plate (three rows of cells) showing ascidian lineage nomenclature. Bars indicate sister relationship between cells. The anteroposterior axis is indicated. The a-line refers to cells from the anterior ectoderm, a8._ indicates cells in the eight generation. A-line indicates the anterior vegetal lineage. (**B**) (Left) Schematic of neural plate at mid-gastrula stage. Rows III-VI derive from a-line neurogenic ectoderm that expresses *DMRT*, and is collectively referred to as anterior neural plate. The *FoxC* expression pattern is shown in green, *ZicL* in pink (note that *ZicL* is also expressed in all cells of rows I and II). A-line cells are yellow. Dashed vertical line indicates the midline; the dashed horizontal line indicates the boundary between presumptive stomodeum (CNS) and palp placode (PNS). (Right) Cis-regulatory DNA upstream of the *DMRT* coding sequence labels anterior neural plate (only the left side of the embryo expresses the *DMRT*>lacZ transgene, which is detected with anti-β-gal antibody, red). Electroporation of plasmids sometimes results in embryos with left-right mosaicism. (**C**) Enhancers for *FoxC* (driving GFP) and *ZicL* (driving mCherry) show the boundary between the palp placode and CNS in gastrula (left) and tailbud (right) stage embryos. (**D**) (Top) Schematic of the tadpole larva nervous system, reflecting the neural plate pattern shown in B; dorsal view. The *FoxC* expression domain (green) marks the palps. The anterior brain (pink) derives from rows III/IV. The stomodeum (dark pink outline) has a rosette arrangement of cells and abuts the anterior brain. Posterior brain and caudal nerve cord (yellow) derive from rows I/II. The dark spots in the brain represent the pigmented otolith and ocellus. (Bottom) Late tailbud stage embryo expressing GFP and RFP driven by the *FoxC* and *DMRT* enhancers. DIC image shows two of the three palps protruding from the anterior end of the trunk. Anterior is to the left. Mosaic inheritance of plasmids reveals *FoxC* staining in the bottom palp and *DMRT* expression in the palp and the left side of the anterior brain. The approximate outline of the brain, both anterior and posterior components, is indicated (blue).

vertebrates, the neural plate is defined on the basis of neurulation to form the CNS; the neurogenic tissues anterior to the plate are called placodes and their neurons contribute to the PNS. Thus, the simple *Ciona* neural plate, as classically defined, includes a neural plate proper as well as a placodal territory (rows V/VI).

The adhesive papillae of the *Ciona* tadpole derive from the a8.18 and a8.20 blastomeres of 112-cell stage embryos, which express the forkhead transcriptional repressor *FoxC* (Imai et al., 2006; Lamy et al., 2006). *FoxC* expression is maintained in the progeny of these cells, namely a9.35, a9.36, a9.39 and a9.40, which comprise the medial four columns of the anteriormost neural plate, rows V and VI (Fig. 1A,B). We have isolated a ~2 kb *FoxC* enhancer upstream of the *FoxC* coding sequence and found it to recapitulate the native expression pattern in gastrula stage embryos (Fig. 1C). Posterior to the a8.18/a8.20 palp precursor cells are the a8.17/a8.19 cells, which contribute to anterior brain and stomodeum. The a8.17/a8.19 blastomeres express *ZicL*, but not *FoxC*. An enhancer for *ZicL* has been described (Shi and Levine, 2008). It drives expression in the a8.19/a8.17 cells, as well as in their lateral neighbor a8.25, and also in the vegetal neural progenitors (rows I/II) and mesodermal lineages (Fig. 1A-C). Thus, *FoxC* and *ZicL* and their enhancers are active in complementary patterns in the anterior neural plate and allow visualization of the boundary between the CNS and PNS.

The *FoxC*-expressing and *ZicL*-expressing cells derive from a common progenitor that expresses *DMRT* (Fig. 1B). Both *FoxC* and *ZicL* require *DMRT* for their activation (Imai et al., 2006; Tresser et al., 2010). *DMRT* is homologous to the *Drosophila doublesex* gene, which, in addition to a role in sex determination, also functions in the development of neurons controlling sex-specific behavior (Rideout et al., 2007; Rideout et al., 2010). In vertebrate embryos, DMRT genes mark anterior neural regions, including the nasal placode and presumptive forebrain (Winkler et al., 2004; Huang et al., 2005; Veith et al., 2006; Wen et al., 2009; Yoshizawa et al., 2011). In *Ciona*, *DMRT* is first expressed at the 64-cell stage in the a7.10, a7.9 and a7.13 blastomeres, which are progenitors of the anterior neural plate (a-line, rows III-VI) (Imai et al., 2006; Tresser et al., 2010). The medial two cells, a7.10 and a7.9, undergo a cell fate choice to produce daughters that express either *ZicL* posteriorly (a8.17/a8.19) or *FoxC* anteriorly (a8.18/a8.20) (see Fig. 1A,B). We have isolated a ~1 kb enhancer upstream of the *DMRT* gene and used this cis-regulatory DNA to perturb gene expression and fluorescently label cells of the anterior neural plate (rows III-VI).

## Differential MAPK activity across the neural plate

What determines the outcome of the *FoxC-ZicL* cell fate choice? The FGF signaling pathway functions in multiple cell fate choice events during nervous system development in *Ciona* embryos (Hudson et al., 2007; Picco et al., 2007; Stolfi and Levine, 2011; Stolfi et al., 2011). The Map kinase (MAPK) signaling cascade can mediate signal transduction downstream of the FGF receptor, and active MAPK signaling can be detected with an antibody that recognizes a dual-phosphorylated (dp) form of the extracellular regulated kinase 1/2 (ERK1/2) (Yao et al., 2000; Hudson et al., 2003; Hudson et al., 2007). To determine the timing and levels of MAPK activation in developing neural tissue, we stained staged embryos with dpERK antibody. These embryos were electroporated with a *FoxB* reporter plasmid (driving H2B:CFP or GFP) to label the vegetal neural precursors that express FGF9/16/20 (A8.7, 8.8, 8.15, 8.16) (Imai et al., 2002; Tassy et al., 2010); this also assists in correct identification of the cells of interest.

Shortly after the cell fate choice, at ~4.75 hpf, we detected dpERK staining in both the *FoxC*-expressing and *ZicL*-expressing cells, as well as in the mother cells on the right-hand side of the embryo, which have yet to divide (Fig. 2Aa,b). The level of staining appeared uniform in all nuclei. By contrast, when we looked a little later in the cell cycle, at 5.17 hpf, we noticed that the dpERK signal appeared graded (Fig. 2Ba,c,d). The strongest signal was seen in the vegetal A-line neural cells, in which it appeared to be both nuclear and cytoplasmic. In the a8.17/a8.19 cells, however, the dpERK signal was concentrated in the nuclei, whereas the anteriormost *FoxC*-expressing cells, a8.18 and a8.20, showed no detectable staining. The non-neural ectoderm adjacent to the *FoxC*-expressing cells showed elevated staining, comparable to that seen in the A-line neural cells. As a control, we stained embryos treated with the MAPK pathway inhibitor U0126, and found that the dpERK antibody signal was abolished (supplementary material Fig. S1). These results suggest that the level of MAPK activation is differentially regulated between the *FoxC*-expressing and *ZicL*-expressing cells, and might be an important factor in determining the downstream gene expression program.

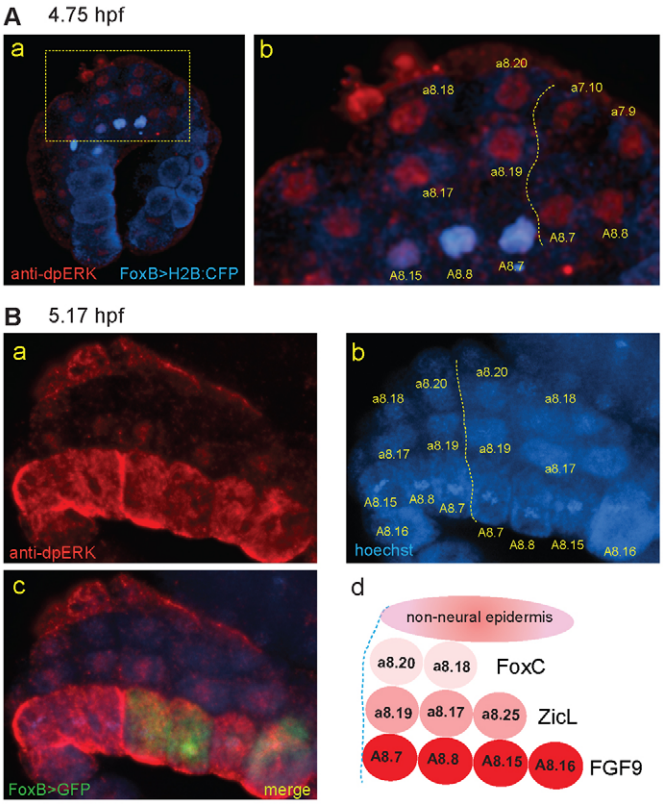


**Fig. 2. A gradient of dpERK staining across the nascent neural plate.** *Ciona* embryos were electroporated with plasmid containing a *FoxB* enhancer driving H2B:CFP (A) or GFP (B) to label the vegetal neural precursors that express FGF9/16/20. Embryos were fixed at 4.75 (A) or 5.17 hpf (B) and stained with dpERK antibody and Hoechst. (**A**) dpERK signal shows uniform intensity in the a-line cells a8.17, a8.18, a8.19 and a8.20. The boxed region in b is magnified in a. Dotted line indicates the midline; the a7.10 and a7.9 blastomeres on the right side of the embryo have not yet divided. Only the left side of the embryo expresses the *FoxB* transgene. (**B**) dpERK signal shows graded distribution in neural precursors. The vegetal neural cells, expressing the *FoxB*>GFP reporter (on the right side only in c), show the strongest signal. Nuclear dpERK is detected in the a8.17 and a8.19 blastomeres (which express *ZicL*), but not in the palp precursor cells. Elevated staining levels are seen in the non-neural ectoderm bordering the *FoxC*-expressing cells. (d) Schematic of dpERK gradient in neural precursors at the 112-cell stage.

## FGF-MAPK signaling is required for differential *FoxC* and *ZicL* expression

The localized dpERK we observed in the *ZicL*-expressing cells is consistent with reports that FGF-MAPK signaling is important for its activation (Imai et al., 2006). We perturbed FGF-MAPK signaling by misexpressing a dominant-negative FGF receptor (DN-FGFR, which lacks the intracellular tyrosine kinase domain) using the *DMRT 5′* enhancer and assayed the activity of the *ZicL* and *FoxC* enhancers. Although the cell fate choice is complete at the 112-cell stage, we assayed expression at mid-gastrula stage because the shape of the embryo makes it easier to visualize the cells of interest. DN-FGFR expression led to loss of *ZicL* in rows III/IV of the neural plate, although sometimes cells in the lateral-most columns escaped repression (compare Fig. 3Aa with 3Ab). Additionally, we observed ectopic expression of *FoxC* in rows III/IV of the neural plate, as compared with the control, in which *FoxC* is expressed only in rows V and VI (compare Fig. 3Ac with 3Ad). To confirm this result, we used the irreversible MAPK pathway inhibitor U0126 to block the MAPK signaling cascade downstream of the FGF receptor, and examined the expression of *FoxC* and *ZicL* transcripts. As with DN-FGFR, U0126 treatment led to loss of *ZicL* in rows III and IV (compare Fig. 3Ba with 3Bb), concomitant with ectopic *FoxC* expression (compare Fig. 3Bc with 3Bd). Expression of a constitutively active (CA) form of FGFR had no effect on the *FoxC* expression pattern. However, co-expression of CA-FGFR and DN-FGFR was able to rescue the ectopic *FoxC* pattern observed with DN-FGFR alone (supplementary material Fig. S2). We conclude that FGF-MAPK signaling is required for *ZicL* expression and for setting the posterior boundary of the *FoxC* expression domain.

## FGF-MAPK signaling is required for patterning of the anterior neural plate

We next asked whether abrogation of MAPK signaling had a broader impact on neural plate patterning, beyond altered expression of *FoxC* and *ZicL*. *Ephrin A-d*, which encodes a membrane-localized signaling molecule, is co-expressed with *FoxC* in rows V and VI of the neural plate. Upon U0126 treatment,

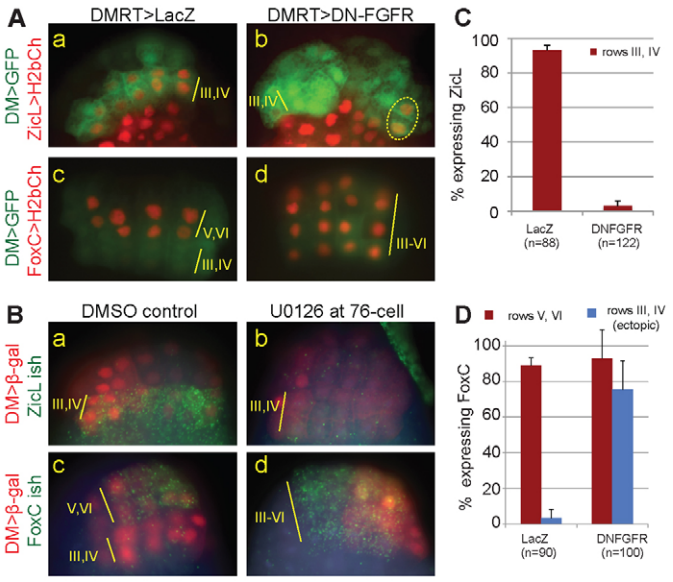


**Fig. 3. FGF-MAPK signaling is required for *ZicL* expression in rows III and IV of the neural plate, and its inhibition leads to ectopic *FoxC* expression.** (**A**) *ZicL* (a,b) and *FoxC* (c,d) enhancer activity in the presence of dominant-negative FGF receptor or a *lacZ* control, driven by the *DMRT* enhancer. Images focus on rows III-VI of the neural plate, which are labeled with *DMRT*>GFP. DN-FGFR leads to loss of *ZicL* from rows III/IV (compare a with b) and to ectopic expression of *FoxC* in rows III/IV (compare c with d). Sometimes, *ZicL* was not repressed in the lateral-most cells of rows III/IV (dotted oval). (**B**) Double in situ hybridization (ish) and antibody staining of embryos treated with the MEK inhibitor U0126 at the 76-cell stage (just prior to the cell fate choice between *FoxC* and *ZicL*). Images focus on rows III-VI, which are labeled with *DMRT*>lacZ and stained with β-gal antibody (red). (a,b) The *ZicL* transcript is lost from rows III/IV upon U0126 treatment. (c,d) *FoxC* in situ hybridization shows ectopic expression in rows III/IV in the presence of U0126. Note the mosaic inheritance of the *DMRT*>lacZ plasmid in d. Nuclei are stained with Hoechst. (**C**,**D**) Quantification of data from A. Error bars indicate s.d.

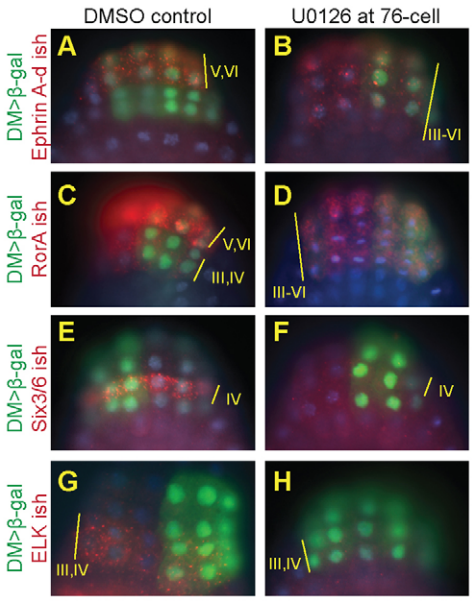


**Fig. 4. MAPK signaling is required to pattern rows III and IV of the neural plate.** Double in situ hybridization and antibody staining in *Ciona* embryos expressing *DMRT*>lacZ (detected with β-gal antibody, green), with and without U0126 treatment at the 76-cell stage. Note that embryos in B-D,F,G show mosaic inheritance of the plasmid primarily on the right-hand side. Endogenous transcripts were detected with DIG-labeled probes via tyramide amplification with Cy3 (red). Nuclei were stained with Hoechst. (**A**,**B**) The row V/VI marker *Ephrin A-d* expands to rows III and IV upon U0126 treatment. (**C**,**D**) *RorA* shows strong expression in rows V/VI and weaker signal in rows III/IV under control conditions, but the pattern becomes uniform across rows III-VI with U0126 treatment. (**E-H**) The row IV marker *Six3/6* (E,F) and the row III/IV marker *ELK* (G,H) are lost upon U0126 treatment.

however, the *Ephrin A-d* expression pattern expands to include rows III and IV, as does *FoxC* (Fig. 4A,B). *RorA*, which encodes an orphan receptor tyrosine kinase (RTK) that modulates non-canonical Wnt signaling, shows a graded pattern with strong expression in rows V/VI and weaker signal in rows III/IV (Fig. 4C) (Auger et al., 2009). U0126 treatment disturbs the graded nature of the *RorA* pattern, which becomes uniform across rows III-VI (Fig. 4C,D). *Six3/6*, which encodes a homeodomain transcription factor, is normally expressed in row IV of the neural plate (Moret et al., 2005; Christiaen et al., 2007), but its expression is lost upon U0126 treatment (Fig. 4E,F). Likewise, the Ets family transcription factor gene *ELK*, a marker for rows III/IV, is lost with U0126 treatment (Fig. 4G,H). These results indicate that the MAPK signaling cascade is broadly required for proper neural plate patterning, in particular to establish the proper identity of cells in rows III and IV. These cells give rise to the anteriormost derivatives of the CNS, including the anterior brain and stomodeum.

## FoxC can repress *ZicL* expression in the anterior neural plate

Because inhibition of FGF-MAPK signaling led to ectopic *FoxC* and loss of *ZicL* expression, and because the lateral-most cells a9.49/a9.50 do not experience ectopic *FoxC* and sometimes escape repression of *ZicL*, we asked whether FoxC itself might repress *ZicL*. FoxC is known to act as a transcriptional repressor in various metazoans by virtue of a conserved Engrailed homology repressor domain (Yaklichkin et al., 2007). Interestingly, this conserved repressor motif is absent from the *Ciona FoxC* ortholog. Nonetheless, when full-length FoxC protein was misexpressed using the *DMRT* enhancer, *ZicL* was lost from rows III and IV (Fig. 5A). A truncated form of FoxC that lacks the C-terminal 293 amino acids downstream of the forkhead DNA-binding domain was also sufficient to repress *ZicL* (data not shown). These results suggest that, despite lacking an obvious transcriptional repression motif, FoxC can inhibit *ZicL* expression. Whether the repressive effect of FoxC on *ZicL* is direct or indirect will require further study.

We then asked whether ZicL could repress *FoxC* expression, reasoning that a mechanism of mutual repression could account for the establishment of the boundary between rows IV and V of the neural plate. However, misexpression of *ZicL* had no effect on the endogenous *FoxC* expression pattern (Fig. 5B). We verified this result by misexpressing *ZicL* with the *Bmp2b* enhancer, which is active much earlier, at the 16-cell stage, and should allow sufficient time to accumulate transgene expression (Christiaen et al., 2009a). Again, ectopic *ZicL* expression had no effect on *FoxC* (data not shown).

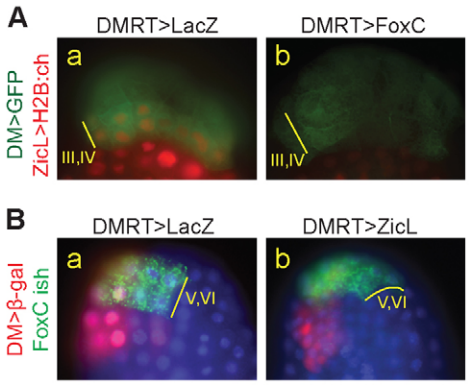


**Fig. 5. *FoxC* promotes the repression of *ZicL*, but not vice versa.** (**A**) *ZicL* enhancer activity in rows III/IV is lost when *FoxC* is misexpressed using the *DMRT* enhancer (b) as compared with control (*lacZ* expression, a). (**B**) Double in situ hybridization and antibody staining. *DMRT*>lacZ labels rows III-VI, as revealed by β-gal antibody staining (red); nuclei are stained with Hoechst. Note the mosaic inheritance of plasmids as revealed by β-gal staining primarily on the left side of the embryo. *FoxC* transcript (green) is detected in rows V/VI in the control condition (a) and is unaffected by ectopic *ZicL* expression driven by the *DMRT* enhancer (b).

## *FoxC* cis-regulatory analysis

How does MAPK signaling keep *FoxC* repressed in rows III/IV of the neural plate? Ets family transcription factors are known effectors of FGF-MAPK signaling and can act as transcriptional repressors in various contexts (Oikawa and Yamada, 2003; Hollenhorst et al., 2011). We identified a 'minimal' *FoxC* enhancer by making 5′ and 3′ deletions of the original 2 kb fragment, to facilitate analysis of potential transcription factor binding sites. We isolated a 325 bp fragment that maps from –375 to –50 bp relative to the start codon, and cloned it upstream of a heterologous promoter (Rothbacher et al., 2007) (from the *FOG* gene) to drive *lacZ* expression. This minimal *FoxC* enhancer is conserved in the related species *C. savignyi* and was sufficient to drive a wild-type *FoxC* expression pattern (Fig. 6B).

We then searched for Ets sites in the minimal *FoxC* enhancer. Ets family transcription factors recognize a well-defined core consensus sequence: GGAA/T (Hollenhorst et al., 2011). We found two candidate sites that map to –255 bp and –295 bp relative to the native start codon and deleted them (Fig. 6A). Deletion of the Ets site at –295 caused an otherwise normal *FoxC-lacZ* fusion gene to exhibit derepressed expression in rows III and IV of the neural plate (Fig. 6B,C). Deletion of the Ets site at –255 had no effect on reporter activity (Fig. 6D). This result suggests that an Ets family transcription factor might repress *FoxC* in rows III/IV of the neural plate.

The *Ciona* genome encodes ~15 Ets domain transcription factors. ELK was an intriguing candidate repressor of *FoxC* because it is expressed in rows III/IV of the neural plate in a MAPK-dependent manner (Fig. 4D). Furthermore, it has been documented that ELK can repress transcription in response to MAPK signaling (Usenko et al., 2002). However, when we misexpressed *ELK* with the *DMRT* enhancer, *FoxC* expression was unaffected (data not shown). Thus, although our data collectively suggest that an Ets family factor might function to repress *FoxC* expression in rows III/IV, the identity of such a factor remains unknown.

## FGF signaling is required for anterior brain development

We next looked at tailbud stage embryos that developed under conditions of perturbed FGF signaling to examine the morphology of the sensory vesicle and palp placode. We predicted that the ectopic *FoxC* might lead to the specification of ectopic palps at the expense of anterior brain. In control embryos, cells of the anterior brain are marked by co-expression of *DMRT* and *ZicL* (pink cells in Fig. 7A), whereas cells expressing *DMRT* but not *ZicL* (row V/VI derivatives) label the anterior trunk ectoderm (palp placode and progeny of a9.51/a9.52; blue cells in Fig. 7A; see also Fig. 1B). In the presence of DN-FGFR, we observe a dramatic expansion of the anterior epidermis at the expense of anterior brain cells, as evidenced by a larger proportion of $DMRT^{+}$ cells lacking *ZicL* expression (Fig. 7B). This was accompanied by an expansion of epidermis marker gene expression (supplementary material Fig. S3). The few remaining cells that co-express *DMRT* and *ZicL* derive from the lateral columns of the neural plate, a9.49/a9.50, which do not experience ectopic *FoxC* when FGF signaling is perturbed (Fig. 3Ad,Bd).

Phalloidin staining of DN-FGFR-expressing tailbud embryos reveals a smaller sensory vesicle, which is rounded rather than elliptical in shape (Fig. 7C,D). This truncated brain is entirely derived from vegetal neural plate cells, as evidenced by the lack of

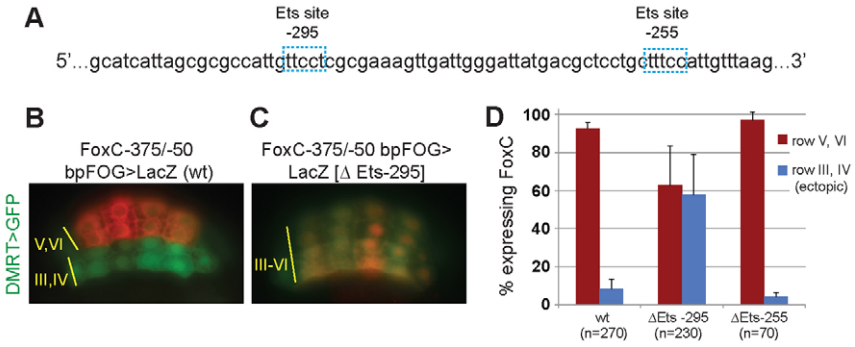


**Fig. 6. An Ets binding site in a minimal *FoxC* enhancer is required to repress expression in rows III and IV of the neural plate.** (**A**) Partial sequence of a minimal *FoxC* enhancer showing two putative Ets binding sites (blue boxes). (**B**) *Ciona* embryos were electroporated with plasmids *DMRT*>GFP to label the anterior neural plate and a *FoxC* minimal enhancer fragment (FoxC –375/–50 bp) cloned upstream of a heterologous promoter (from the *FOG* gene) driving *lacZ*. *lacZ* expression was detected by immunostaining with β-gal antibody (red). (**C**) Expression pattern of the minimal *FoxC* enhancer fragment from which the Ets site at –295 had been deleted. (**D**) Quantification of the results shown in B,C. Error bars indicate s.d. wt, wild type.

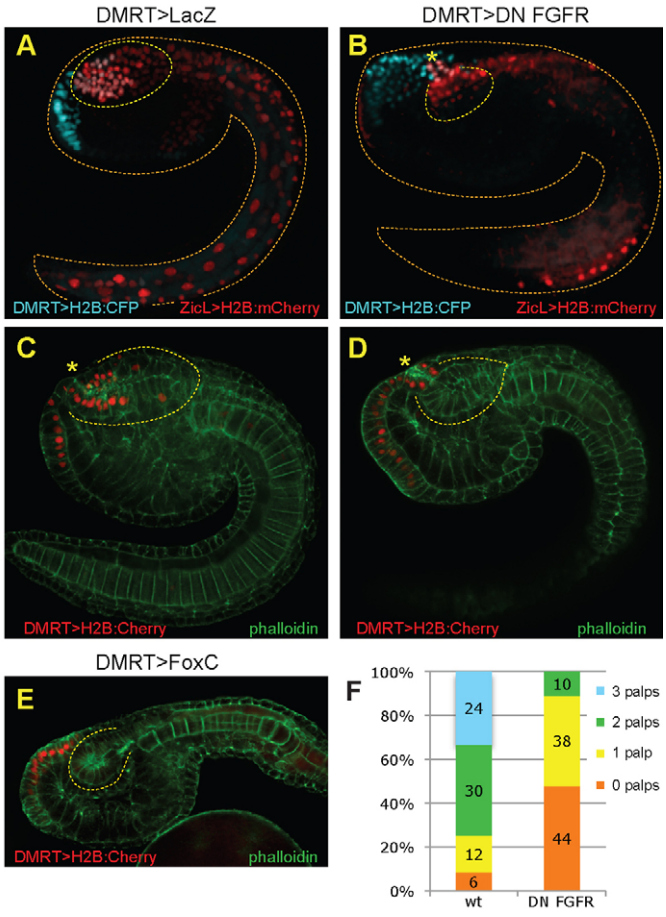


**Fig. 7. FGF signaling delineates the boundary between the anterior neural tube and the palp placode.** (**A**,**B**) Tailbud stage *Ciona* embryos electroporated with plasmids *DMRT*>H2B:CFP and *ZicL*>H2B:mCherry, in the presence of *DMRT*>DN-FGFR or *DMRT*>lacZ as control. Anterior brain cells are marked by co-expression of *ZicL* and *DMRT* reporters (pink cells); cells expressing only the *DMRT* reporter derive from rows V/VI of the neural plate. DN-FGFR expression leads to loss of cells in the anterior brain, as compared with control. (**C**,**D**) Tailbud embryos were electroporated with *DMRT*>H2B:mCherry plasmid and stained with phalloidin. The brain shows an anterior truncation in the presence of DN-FGFR, but the neuropore still forms, albeit shifted posteriorly. (**E**) Tailbud embryo expressing *DMRT*>FoxC transgene shows truncation of anterior neural tube, similar to D. (**F**) Larvae expressing *DMRT*>DNFGFR were compared with controls expressing *DMRT*>lacZ and the number of palps was counted. The brain vesicle is outlined; asterisk indicates the neuropore.

*DMRT* expression (Fig. 7D). *DMRT*$^{+}$ cells remain on the surface of the embryo, rather than being internalized to form the brain vesicle (compare *DMRT* pattern in Fig. 7C and 7D). Interestingly, we observed a neuropore positioned on top of the truncated brain; note that this neuropore is shifted posteriorly compared with that of the control (asterisks, Fig. 7C,D). Taken together, these results suggest that, normally, the boundary between the palp placode and the CNS corresponds to the boundary between the *FoxC* and *ZicL* expression domains. Shifting the domain of *FoxC* expression posteriorly induces a similar posterior shift of the palp placode.

We next looked at tailbud embryos misexpressing *FoxC* to determine whether this manipulation recapitulates the DN-FGFR phenotype. Fig. 7E shows that *FoxC* misexpression indeed leads to truncation of the anterior brain (compare Fig. 7D and 7E), suggesting that *FoxC* expression is sufficient to promote a placodal rather than CNS cell fate. The *FoxC*-misexpressing cells, labeled with the *DMRT* reporter, remain in a columnar epithelium on the dorso-anterior surface of the embryo. Notably, we found no evidence of anterior neuropore formation. The *DMRT* enhancer drives *FoxC* expression across all six columns of the anterior neural plate, whereas the DN-FGFR perturbation leads to ectopic *FoxC* only in the medial four columns. This suggests that proper specification of the lateral-most columns of the neural plate, in part through exclusion of *FoxC*, is necessary for neuropore formation (Nicol and Meinertzhagen, 1988).

Ectopic expression of *FoxC* via inhibition of FGF signaling does not cause transformation of the anterior brain into supernumerary palps. On the contrary, palp development is impaired (Fig. 7F). This is in agreement with a previous study showing that MAPK signaling is required at least through neurula stages for proper palp development (Hudson et al., 2003). Thus, although *FoxC* is a marker of the palp lineage, its expression alone does not suffice to direct morphogenesis of the palps. Our results show that abrogation of MAPK signaling causes a posterior shift in the boundary between the palp placode and the presumptive stomodeum, and suggest that *FoxC* expression might function in part to position the anterior neuropore (see below).

## DISCUSSION

We have presented evidence that FGF-MAPK signaling is required to specify anterior CNS fates (*ZicL*) in rows III/IV of the neural plate, and that disruption of this pathway causes derepression of *FoxC*, which is normally restricted to rows V/VI (Fig. 3). Inhibition of FGF-MAPK signaling also causes the loss of other determinants of the anterior neural tube, including *Six3/6*, which marks the presumptive stomodeum (Fig. 4) (Mazet and Shimeld, 2005; Christiaen et al., 2007). A similar situation is seen in the posterior neural plate comprising rows I/II, which derive from the vegetal A-line and contribute to the posterior CNS, including the motor ganglion and caudal nerve cord. Hudson et al. showed that MAPK signaling is required for the expression of row I markers such as *Mnx*, *Cdx* and *Ephrin A-b*; the loss of row I markers in U0126-treated embryos was accompanied by the posterior expansion of row II markers into row I (Hudson et al., 2007). Thus, FGF-MAPK signaling broadly promotes posterior cell fates over anterior cell fates across the developing nervous system in *Ciona*. This trend is also seen in vertebrates, where neural induction generally promotes nervous tissue of anterior character and FGF signaling acts on this specified tissue to induce posterior fates (Gamse and Sive, 2000; Ribisi et al., 2000; Stern, 2001; Dono, 2003; Fletcher et al., 2006).

*FoxC* maintains differential expression of *ZicL* and *FoxC* by inhibiting *ZicL* expression in rows V and VI. Ectopic expression of *FoxC* in rows III and IV results in the loss of *ZicL*. Thus, regulatory interactions between *FoxC* and *ZicL* appear to be hierarchical, rather than mutual. That is, *FoxC* inhibits *ZicL*, but misexpression of *ZicL* in rows V and VI does not alter the expression of *FoxC* (Fig. 5). Hierarchical repression is observed in the dorsal-ventral patterning of the *Drosophila melanogaster* CNS, with ventral repressors such as Snail and Vnd inhibiting the expression of more dorsal determinants such as Ind and Msh (Drop), but not vice versa (Cowden and Levine, 2003). By contrast, anterior-posterior patterning depends on mutual cross-repression, particularly among pairs of gap genes (*hunchback*/*knirps* and *giant*/*Kruppel*) (Kraut and Levine, 1991).

The palps derive from an embryonic territory sandwiched between the non-neural ectoderm and progenitors of the CNS (stomodeum and anterior brain). The corresponding region in vertebrate embryos forms the anterior placodes, which give rise to the lens, olfactory epithelium and adenohypophysis (anterior pituitary) (Streit, 2008; Schlosser, 2010). In chick embryos, *FoxC* is expressed in the lens placode, and in mammals it functions in the development of the anterior eye (Saleem et al., 2003; Bailey et al., 2006; Berry et al., 2006). *FoxC* is also expressed in the developing *Xenopus* eye, although it is not clear whether this expression is in the lens placode and/or the surrounding tissue (Bowes et al., 2010). It is noteworthy that FGF signaling functions in the chick to repress lens fate and promote olfactory placode development (Bailey et al., 2006). A parallel situation is seen in the *Ciona* palp placode, which expresses *FoxC* and β/γ-crystallin, another lens marker (Shimeld et al., 2005), and is repressed by FGF signaling.

We do not suggest homology of the *Ciona* palp placode with the vertebrate lens placode. *Ciona* has a light-sensing apparatus that consists of a pigmented ocellus and numerous photoreceptor cells, and these are located in the anterior brain (Imai and Meinertzhagen, 2007a; Horie et al., 2008). The palp placode also expresses olfactory placode markers such as *DMRT*, *Coe* and *Dlx* genes (Caracciolo et al., 2000; Winkler et al., 2004; Huang et al., 2005; Mazet et al., 2005; Veith et al., 2006; Wen et al., 2009). Thus, we refer to the *Ciona* palp primordium simply as an anterior placode, which might be derived from an ancestral structure that evolved into separate, specialized anterior placodes in the vertebrate lineage.

In summary, the boundary between rows IV and V of the *Ciona* neural plate is important because it delineates the neural tube as distinct from the anterior placode region. We have shown that FGF-MAPK signaling is required to establish this boundary and that it does so by repressing *FoxC* expression in the presumptive brain. Disruption of FGF signaling leads to a truncated anterior brain, reminiscent of the phenotype of triple FGFR knockout mice, which lack the telencephalon (Paek et al., 2009). *Ciona* embryos develop from defined cell lineages, and the gene expression patterns that underlie important embryological boundaries form relatively early in development. In vertebrates, neural territories are composed of mixed fate cell populations, which segregate and form boundaries according to fate at comparatively later developmental stages in response to diverse signals, including FGFs (Puelles et al., 2005; Toro and Varga, 2007; Cajal et al., 2012; Sanchez-Arrones et al., 2012). Despite these differences, a common requirement for FGF signaling highlights the relevance of *Ciona* embryos to the study of patterning and the morphogenetic mechanisms underlying vertebrate development.

**Acknowledgements**
We thank Alberto Stolfi for critical reading of the manuscript and sharing many reagents and Lionel Christiaen for helpful comments and the *Bmp2b*>ZicL plasmid.

**Funding**
This work was supported by an American Cancer Society California Division Campaign for Research Postdoctoral Fellowship (to E.W.).

**Competing interests statement**
The authors declare no competing financial interests.

**Supplementary material**
Supplementary material available online at
http://dev.biologists.org/lookup/suppl/doi:10.1242/dev.078485/-/DC1

**References**

**Auger, H., Lamy, C., Haeussler, M., Khoueiry, P., Lemaire, P. and Joly, J. S.** (2009). Similar regulatory logic in Ciona intestinalis for two Wnt pathway modulators, ROR and SFRP-1/5. *Dev. Biol.* **329**, 364-373.
**Bailey, A. P., Bhattacharyya, S., Bronner-Fraser, M. and Streit, A.** (2006). Lens specification is the ground state of all sensory placodes, from which FGF promotes olfactory identity. *Dev. Cell* **11**, 505-517.
**Berry, F. B., Lines, M. A., Oas, J. M., Footz, T., Underhill, D. A., Gage, P. J. and Walter, M. A.** (2006). Functional interactions between FOXC1 and PITX2 underlie the sensitivity to FOXC1 gene dose in Axenfeld-Rieger syndrome and anterior segment dysgenesis. *Hum. Mol. Genet.* **15**, 905-919.
**Bertrand, V., Hudson, C., Caillol, D., Popovici, C. and Lemaire, P.** (2003). Neural tissue in ascidian embryos is induced by FGF9/16/20, acting via a combination of maternal GATA and Ets transcription factors. *Cell* **115**, 615-627.
**Bowes, J. B., Snyder, K. A., Segerdell, E., Jarabek, C. J., Azam, K., Zorn, A. M. and Vize, P. D.** (2010). Xenbase: gene expression and improved integration. *Nucleic Acids Res.* **38**, D607-D612.
**Cajal, M., Lawson, K. A., Hill, B., Moreau, A., Rao, J., Ross, A., Collignon, J. and Camus, A.** (2012). Clonal and molecular analysis of the prospective anterior neural boundary in the mouse embryo. *Development* **139**, 423-436.
**Caracciolo, A., Di Gregorio, A., Aniello, F., Di Lauro, R. and Branno, M.** (2000). Identification and developmental expression of three Distal-less homeobox containing genes in the ascidian Ciona intestinalis. *Mech. Dev.* **99**, 173-176.
**Christiaen, L., Jaszczyszyn, Y., Kerfant, M., Kano, S., Thermes, V. and Joly, J. S.** (2007). Evolutionary modification of mouth position in deuterostomes. *Semin. Cell Dev. Biol.* **18**, 502-511.
**Christiaen, L., Stolfi, A., Davidson, B. and Levine, M.** (2009a). Spatio-temporal intersection of Lhx3 and Tbx6 defines the cardiac field through synergistic activation of Mesp. *Dev. Biol.* **328**, 552-560.
**Christiaen, L., Wagner, E., Shi, W. and Levine, M.** (2009b). Electroporation of transgenic DNAs in the sea squirt Ciona. *Cold Spring Harb. Protoc.* **2009**, pdb prot5345.
**Christiaen, L., Wagner, E., Shi, W. and Levine, M.** (2009c). Isolation of sea squirt (Ciona) gametes, fertilization, dechorionation, and development. *Cold Spring Harb. Protoc.* **2009**, pdb prot5344.
**Christiaen, L., Wagner, E., Shi, W. and Levine, M.** (2009d). Whole-mount in situ hybridization on sea squirt (Ciona intestinalis) embryos. *Cold Spring Harb. Protoc.* **2009**, pdb prot5348.
**Conklin, E. G.** (1905). The organization and cell-lineage of the ascidian egg. *J. Acad. Nat. Sci. (Philadelphia)* **13**, 1-119.
**Cowden, J. and Levine, M.** (2003). Ventral dominance governs sequential patterns of gene expression across the dorsal-ventral axis of the neuroectoderm in the Drosophila embryo. *Dev. Biol.* **262**, 335-349.
**Davidson, B., Shi, W., Beh, J., Christiaen, L. and Levine, M.** (2006). FGF signaling delineates the cardiac progenitor field in the simple chordate, Ciona intestinalis. *Genes Dev.* **20**, 2728-2738.
**Dehal, P. and Boore, J. L.** (2005). Two rounds of whole genome duplication in the ancestral vertebrate. *PLoS Biol.* **3**, e314.
**Delaune, E., Lemaire, P. and Kodjabachian, L.** (2005). Neural induction in Xenopus requires early FGF signalling in addition to BMP inhibition. *Development* **132**, 299-310.
**Delsuc, F., Brinkmann, H., Chourrout, D. and Philippe, H.** (2006). Tunicates and not cephalochordates are the closest living relatives of vertebrates. *Nature* **439**, 965-968.
**Dono, R.** (2003). Fibroblast growth factors as regulators of central nervous system development and function. *Am. J. Physiol. Regul. Integr. Comp. Physiol.* **284**, R867-R881.
**Fletcher, R. B., Baker, J. C. and Harland, R. M.** (2006). FGF8 spliceforms mediate early mesoderm and posterior neural tissue formation in Xenopus. *Development* **133**, 1703-1714.
**Gamse, J. and Sive, H.** (2000). Vertebrate anteroposterior patterning: the Xenopus neurectoderm as a paradigm. *BioEssays* **22**, 976-986.
**Harafuji, N., Keys, D. N. and Levine, M.** (2002). Genome-wide identification of tissue-specific enhancers in the Ciona tadpole. *Proc. Natl. Acad. Sci. USA* **99**, 6802-6805.
**Hollenhorst, P. C., McIntosh, L. P. and Graves, B. J.** (2011). Genomic and biochemical insights into the specificity of ETS transcription factors. *Annu. Rev. Biochem.* **80**, 437-471.
**Horie, T., Sakurai, D., Ohtsuki, H., Terakita, A., Shichida, Y., Usukura, J., Kusakabe, T. and Tsuda, M.** (2008). Pigmented and nonpigmented ocelli in the brain vesicle of the ascidian larva. *J. Comp. Neurol.* **509**, 88-102.
**Huang, X., Hong, C. S., O'Donnell, M. and Saint-Jeannet, J. P.** (2005). The doublesex-related gene, XDmrt4, is required for neurogenesis in the olfactory system. *Proc. Natl. Acad. Sci. USA* **102**, 11349-11354.
**Hudson, C., Darras, S., Caillol, D., Yasuo, H. and Lemaire, P.** (2003). A conserved role for the MEK signalling pathway in neural tissue specification and posteriorisation in the invertebrate chordate, the ascidian Ciona intestinalis. *Development* **130**, 147-159.

**Hudson, C., Lotito, S. and Yasuo, H.** (2007). Sequential and combinatorial inputs from Nodal, Delta2/Notch and FGF/MEK/ERK signalling pathways establish a grid-like organisation of distinct cell identities in the ascidian neural plate. *Development* **134**, 3527-3537.
**Imai, J. H. and Meinertzhagen, I. A.** (2007a). Neurons of the ascidian larval nervous system in Ciona intestinalis: I. Central nervous system. *J. Comp. Neurol.* **501**, 316-334.
**Imai, J. H. and Meinertzhagen, I. A.** (2007b). Neurons of the ascidian larval nervous system in Ciona intestinalis: II. Peripheral nervous system. *J. Comp. Neurol.* **501**, 335-352.
**Imai, K. S., Satoh, N. and Satou, Y.** (2002). Early embryonic expression of FGF4/6/9 gene and its role in the induction of mesenchyme and notochord in Ciona savignyi embryos. *Development* **129**, 1729-1738.
**Imai, K. S., Levine, M., Satoh, N. and Satou, Y.** (2006). Regulatory blueprint for a chordate embryo. *Science* **312**, 1183-1187.
**Imai, K. S., Stolfi, A., Levine, M. and Satou, Y.** (2009). Gene regulatory networks underlying the compartmentalization of the Ciona central nervous system. *Development* **136**, 285-293.
**Kraut, R. and Levine, M.** (1991). Mutually repressive interactions between the gap genes giant and Kruppel define middle body regions of the Drosophila embryo. *Development* **111**, 611-621.
**Lamy, C., Rothbacher, U., Caillol, D. and Lemaire, P.** (2006). Ci-FoxA-a is the earliest zygotic determinant of the ascidian anterior ectoderm and directly activates Ci-sFRP1/5. *Development* **133**, 2835-2844.
**Lemaire, P., Bertrand, V. and Hudson, C.** (2002). Early steps in the formation of neural tissue in ascidian embryos. *Dev. Biol.* **252**, 151-169.
**Manni, L., Lane, N. J., Joly, J. S., Gasparini, F., Tiozzo, S., Caicci, F., Zaniolo, G. and Burighel, P.** (2004). Neurogenic and non-neurogenic placodes in ascidians. *J. Exp. Zool. B Mol. Dev. Evol.* **302**, 483-504.
**Manni, L., Agnoletto, A., Zaniolo, G. and Burighel, P.** (2005). Stomodeal and neurohypophysial placodes in Ciona intestinalis: insights into the origin of the pituitary gland. *J. Exp. Zool. B Mol. Dev. Evol.* **304**, 324-339.
**Mazet, F. and Shimeld, S. M.** (2005). Molecular evidence from ascidians for the evolutionary origin of vertebrate cranial sensory placodes. *J. Exp. Zool. B Mol. Dev. Evol.* **304**, 340-346.
**Mazet, F., Hutt, J. A., Milloz, J., Millard, J., Graham, A. and Shimeld, S. M.** (2005). Molecular evidence from Ciona intestinalis for the evolutionary origin of vertebrate sensory placodes. *Dev. Biol.* **282**, 494-508.
**Meinertzhagen, I. A., Lemaire, P. and Okamura, Y.** (2004). The neurobiology of the ascidian tadpole larva: recent developments in an ancient chordate. *Annu. Rev. Neurosci.* **27**, 453-485.
**Moret, F., Christiaen, L., Deyts, C., Blin, M., Vernier, P. and Joly, J. S.** (2005). Regulatory gene expressions in the ascidian ventral sensory vesicle: evolutionary relationships with the vertebrate hypothalamus. *Dev. Biol.* **277**, 567-579.
**Nicol, D. and Meinertzhagen, I. A.** (1988). Development of the central nervous system of the larva of the ascidian, Ciona intestinalis L. II. Neural plate morphogenesis and cell lineages during neurulation. *Dev. Biol.* **130**, 737-766.
**Oikawa, T. and Yamada, T.** (2003). Molecular biology of the Ets family of transcription factors. *Gene* **303**, 11-34.
**Paek, H., Gutin, G. and Hebert, J. M.** (2009). FGF signaling is strictly required to maintain early telencephalic precursor cell survival. *Development* **136**, 2457-2465.
**Passamaneck, Y. J. and Di Gregorio, A.** (2005). Ciona intestinalis: chordate development made simple. *Dev. Dyn.* **233**, 1-19.
**Picco, V., Hudson, C. and Yasuo, H.** (2007). Ephrin-Eph signalling drives the asymmetric division of notochord/neural precursors in Ciona embryos. *Development* **134**, 1491-1497.
**Puelles, L., Fernandez-Garre, P., Sanchez-Arrones, L., Garcia-Calero, E. and Rodriguez-Gallardo, L.** (2005). Correlation of a chicken stage 4 neural plate fate map with early gene expression patterns. *Brain Res. Brain Res. Rev.* **49**, 167-178.
**Ribisi, S., Jr, Mariani, F. V., Aamar, E., Lamb, T. M., Frank, D. and Harland, R. M.** (2000). Ras-mediated FGF signaling is required for the formation of posterior but not anterior neural tissue in Xenopus laevis. *Dev. Biol.* **227**, 183-196.
**Rideout, E. J., Billeter, J. C. and Goodwin, S. F.** (2007). The sex-determination genes fruitless and doublesex specify a neural substrate required for courtship song. *Curr. Biol.* **17**, 1473-1478.
**Rideout, E. J., Dornan, A. J., Neville, M. C., Eadie, S. and Goodwin, S. F.** (2010). Control of sexual differentiation and behavior by the doublesex gene in Drosophila melanogaster. *Nat. Neurosci.* **13**, 458-466.
**Rothbacher, U., Bertrand, V., Lamy, C. and Lemaire, P.** (2007). A combinatorial code of maternal GATA, Ets and beta-catenin-TCF transcription factors specifies and patterns the early ascidian ectoderm. *Development* **134**, 4023-4032.
**Saleem, R. A., Banerjee-Basu, S., Berry, F. B., Baxevanis, A. D. and Walter, M. A.** (2003). Structural and functional analyses of disease-causing missense mutations in the forkhead domain of FOXC1. *Hum. Mol. Genet.* **12**, 2993-3005.
**Sanchez-Arrones, L., Stern, C. D., Bovolenta, P. and Puelles, L.** (2012). Sharpening of the anterior neural border in the chick by rostral endoderm signalling. *Development* **139**, 1034-1044.
**Satou, Y., Satoh, N. and Imai, K. S.** (2009). Gene regulatory networks in the early ascidian embryo. *Biochim. Biophys. Acta* **1789**, 268-273.
**Schlosser, G.** (2010). Making senses development of vertebrate cranial placodes. *Int. Rev. Cell Mol. Biol.* **283**, 129-234.
**Shi, W. and Levine, M.** (2008). Ephrin signaling establishes asymmetric cell fates in an endomesoderm lineage of the Ciona embryo. *Development* **135**, 931-940.
**Shimeld, S. M., Purkiss, A. G., Dirks, R. P., Bateman, O. A., Slingsby, C. and Lubsen, N. H.** (2005). Urochordate betagamma-crystallin and the evolutionary origin of the vertebrate eye lens. *Curr. Biol.* **15**, 1684-1689.
**Stern, C. D.** (2001). Initial patterning of the central nervous system: how many organizers? *Nat. Rev. Neurosci.* **2**, 92-98.
**Stolfi, A. and Levine, M.** (2011). Neuronal subtype specification in the spinal cord of a protovertebrate. *Development* **138**, 995-1004.
**Stolfi, A., Wagner, E., Taliaferro, J. M., Chou, S. and Levine, M.** (2011). Neural tube patterning by Ephrin, FGF and Notch signaling relays. *Development* **138**, 5429-5439.
**Streit, A.** (2008). The cranial sensory nervous system: specification of sensory progenitors and placodes. In *StemBook*, www.stembook.org.
**Streit, A., Berliner, A. J., Papanayotou, C., Sirulnik, A. and Stern, C. D.** (2000). Initiation of neural induction by FGF signalling before gastrulation. *Nature* **406**, 74-78.
**Tassy, O., Dauga, D., Daian, F., Sobral, D., Robin, F., Khoueiry, P., Salgado, D., Fox, V., Caillol, D., Schiappa, R. et al.** (2010). The ANISEED database: digital representation, formalization, and elucidation of a chordate developmental program. *Genome Res.* **20**, 1459-1468.
**Toro, S. and Varga, Z. M.** (2007). Equivalent progenitor cells in the zebrafish anterior preplacodal field give rise to adenohypophysis, lens, and olfactory placodes. *Semin. Cell Dev. Biol.* **18**, 534-542.
**Tresser, J., Chiba, S., Veeman, M., El-Nachef, D., Newman-Smith, E., Horie, T., Tsuda, M. and Smith, W. C.** (2010). doublesex/mab3 related-1 (dmrt1) is essential for development of anterior neural plate derivatives in Ciona. *Development* **137**, 2197-2203.
**Usenko, T. N., Pospelova, T. V. and Pospelov, V. A.** (2002). Transformation with the E1A + cHa-ras oncogenes enhances the trans-repressor function of the Elk-1 transcription factor. *Molekuliarnaia Biologiia* **36**, 825-832.
**Veeman, M. T., Newman-Smith, E., El-Nachef, D. and Smith, W. C.** (2010). The ascidian mouth opening is derived from the anterior neuropore: reassessing the mouth/neural tube relationship in chordate evolution. *Dev. Biol.* **344**, 138-149.
**Veith, A. M., Schafer, M., Kluver, N., Schmidt, C., Schultheis, C., Schartl, M., Winkler, C. and Volff, J. N.** (2006). Tissue-specific expression of dmrt genes in embryos and adults of the platyfish Xiphophorus maculatus. *Zebrafish* **3**, 325-337.
**Wen, A., You, F., Tan, X., Sun, P., Ni, J., Zhang, Y., Xu, D., Wu, Z., Xu, Y. and Zhang, P.** (2009). Expression pattern of dmrt4 from olive flounder (Paralichthys olivaceus) in adult gonads and during embryogenesis. *Fish Physiol. Biochem.* **35**, 421-433.
**Winkler, C., Hornung, U., Kondo, M., Neuner, C., Duschl, J., Shima, A. and Schartl, M.** (2004). Developmentally regulated and non-sex-specific expression of autosomal dmrt genes in embryos of the Medaka fish (Oryzias latipes). *Mech. Dev.* **121**, 997-1005.
**Yaklichkin, S., Vekker, A., Stayrook, S., Lewis, M. and Kessler, D. S.** (2007). Prevalence of the EH1 Groucho interaction motif in the metazoan Fox family of transcriptional regulators. *BMC Genomics* **8**, 201.
**Yao, Z., Dolginov, Y., Hanoch, T., Yung, Y., Ridner, G., Lando, Z., Zharhary, D. and Seger, R.** (2000). Detection of partially phosphorylated forms of ERK by monoclonal antibodies reveals spatial regulation of ERK activity by phosphatases. *FEBS Lett.* **468**, 37-42.
**Yoshizawa, A., Nakahara, Y., Izawa, T., Ishitani, T., Tsutsumi, M., Kuroiwa, A., Itoh, M. and Kikuchi, Y.** (2011). Zebrafish Dmrta2 regulates neurogenesis in the telencephalon. *Genes Cells* **16**, 1097-1109.